PROCEEDINGS OF SCIENCE

The DAMIC-M experiment: scientific results from prototype detector and development status.

Romain Gaïor[a,*] **for the DAMIC-M collaboration**

[a] *Laboratoire de physique nucléaire et des hautes énergies (LPNHE), Sorbonne Université, Université Paris Cité, CNRS/IN2P3, Paris 75005, France*

E-mail: romain.gaior@lpnhe.in2p3.fr

The DAMIC-M experiment aims at the direct detection of dark matter particle candidates with sub electron resolution Charge Coupled Devices (CCD).
The low energy threshold of a few eV and fine spatial resolution of these so-called skipper CCDs make them a competitive target to search for low mass dark matter candidate. DAMIC-M will search for low mass WIMPs (<5GeV/c^2) through the nuclear recoil they would induce on silicon nuclei but will also probe much lighter candidate such as particles of the hidden sector through the electronic recoil they would provoke.
DAMIC-M in its final stage will comprise 52 CCD modules for a total target mass of around 700 grams and a radioactive background goal of less than 1 event/keV/kg/day. It will be installed in the Modane Underground Laboratory (LSM) in France in 2024.
A prototype detector with 18 grams of target mass, the Low Background Chamber (LBC), has been successfully installed and commissioned in 2022 at LSM and is already giving world leading results in the search for leptophilic dark matter.
We present the first scientific results obtained with the LBC and the status of the development of final DAMIC-M detector.

38th International Cosmic Ray Conference (ICRC2023)
26 July - 3 August, 2023
Nagoya, Japan

*Speaker

PoS(ICRC2023)1419

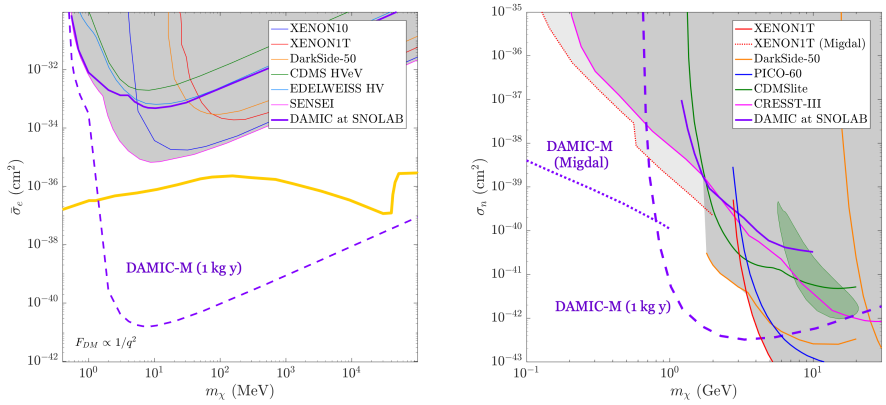

Figure 1: Left: sensitivity estimation for the DM-electron in the case of a light mediator interaction, the yellow curve shows the values giving the right relic abundance. Right: estimation of the DM-nucleus sensitivity for low mass WIMP.

1. Introduction

Search for dark matter (DM) as a new feebly interacting particle is carried over a large range of mass and cross section. If the so called supersymmetric WIMP has been a favored candidate for years, the panorama of experimental searches has recently extended to other models such as the low mass WIMP (with mass below 10GeV/c^2) but also hidden sector model that postulate the existence of a complete non visible sector with DM particle of mass in the MeV/c^2 – GeV/c^2 range [1]. The use of thick fully depleted Charge Coupled Device (CCD) [2] to search for low mass DM has proven to be an efficient technique thanks to a low threshold (few tens of eV) and a controlled radioactive background [3]. The use of skipper CCDs, allows one to even lower the threshold to only a few eV. DAMIC-M will search for low mass DM particles with 700g of skipper CCDs in a low radioactive background setup with an expected rate of less than 1 event/kg/keV/day. The experiment will be located in the Laboratoire Souterrain de Modane (LSM). With such features, DAMIC-M detectors will be able to probe unexplored DM-electron cross section and possibly DM-nucleon cross section as shown in the sensitivity curves of Fig. 1.

2. DM detection with CCD

Upon the interaction of a particle with the bulk silicon of the CCD, if the deposited energy is larger than the energy band gap of 1.12 eV, electron hole pairs cab be produced. The silicon is fully depleted with the appropriate applied substrate voltage. The CCD is divided into pixels by fixed potential applied at regular interval in one direction (the channel stops), and by the potential well formed by the potentials of three clocks. The electric field is used to drift the charges towards a buried channel, a layer at the top surface of the CCD. The lateral spread of the charge packet produced along the drift depends on the depth of the interaction. The pattern of the pixels can also help identifying the particle type that interacted, as it is illustrated in Fig. 2 (left). The charges remain stored during the CCD exposure and are then transferred towards the readout stage of the CCD by changing the clock potentials. The conversion from charge to voltage is done with a field

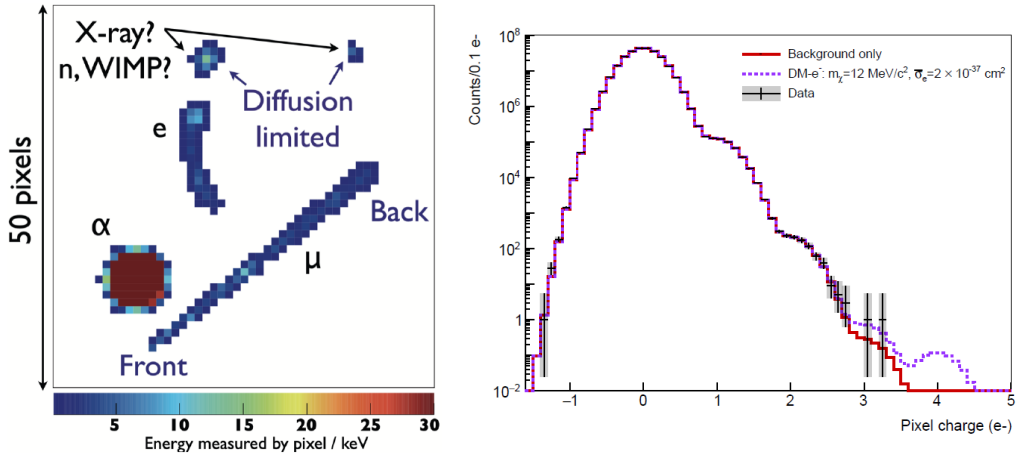

Figure 2: Left: Example of image pattern from different type of particle. Right: Pixel charge distribution used for DM-electron search.

effect transistor, the resulting video signal is amplified and measured by a downstream electronics. The measurement of the charge is affected by the combination of a white noise and a 1/f noise. The skipper CCD technology allows one to repeat the charge measurement without loosing the charge information. One can do short non destructive charge measurements (NDCM) (of the order of 5 to 10 μs each) to avoid 1/f noise and repeat it to decrease the white noise with $\sqrt{NDCM}$. Charge resolutions can be chosen with the number of NDCM and resolution as low as 0.07e$^-$ were obtained with 3000 NDCM. The CCDs have been shown to precisely measured electronic recoil with X ray, γ ray and optical photon down to 40 eV. Recently the DAMIC-M collaboration has also measured precisely the low energy deposit from Compton electron in silicon [14] validating the detector response of the skipper CCD down to 23 eV. As for the yield of ionisation signal upon nuclear recoil, it was measured with a neutron source and amount to around 10% in silicon at 700 eV$_{NR}$ [6].

DAMIC-M will search for nuclear recoils from low mass WIMP in the bulk of the CCD as clusters with limited spatial extension. As the signal from DM has no particular signature, the mitigation and control of radioactive background are key in those searches, an explanation of the adopted strategies is given in the next section. The search for DM-electron interaction from sub-GeV particle is expected to yield only a few charges. Hence those interactions cannot be identified individually but the overall rate of charge in the pixels can be studied to search for signal above the background distribution as shown in Fig. 2 (right). Here the spontaneous emission of charge in the silicon crystal, the dark current, will play a key role in the sensitivity of the detector, as it will be shown in the section 4.

The DAMIC-M CCD are made by 6000 by 1500 pixels of 15 µm x 15 µm and are 675 µm thick. They will be operated at temperatures around 130 K and with a substrate voltage from 40V to 70V. The parameters used to fabricate the CCD were set after the tests of a pre-production batch. The collaboration is also studying the option to remove a layer at the back of the CCD to improve the charge reconstruction from the back of the CCD. The final selection of CCDs will be done according the number of defects, the quality of charge transfer and the noise of the amplifier.

Figure 3: Left: CCDs and pitch adapter. Right: DAMIC-M cryostat, the left hand side pipe is not shown here.

3. DAMIC-M detector

The design of the detector and the choice of the materials used are constrained by the low background requirement of 1 d.r.u. A detailed GEANT4 simulation is used to optimise the design and estimate the final background of the experiment. We also use as a reference the background model developed for the DAMIC at Snolab experiment [9] where it was shown that the main contributions arise from the ^{210}Pb from the CCD surface, the copper material contaminated with ^{210}Pb and Cobalt isotopes from copper activation, the tritium from silicon activation and the ^{32}Si present in the CCD bulk, and finally the detector material such as the flex cable used to convey the electrical signal to the CCD. Specific strategies are adopted depending on the type of background. To cope with the external backgrounds, the CCDs will be installed in a copper cryostat shielded from the gamma background by 25 cm of lead and from the neutron background with 30 cm of high density polyethylene. The design of the experiment is partly shown in Fig. 3 (right). The experiment will be installed at the LSM with a 4800 meter water equivalent overburden which results in about 3.4 muon/m^2/day. The sensitive part is composed of 52 CCD modules, each of them made with 4 CCDs on a pitch adapter. The modules are grouped by 13 and the 4 groups are arranged at right angle with respect to the next one. A special care is taken from the initial procurement of the silicon ingot until the installation of the CCDs to limit the exposition to cosmic ray. For instance, a dedicated shielding was provided to the companies involved in the chain of fabrication of the CCDs to store the silicon material between the phases of fabrication. Also, the transportation of the silicon is done at see level (on truck and ship) in a thick stainless steel shielding. The CCDs will be glued on the pitch adapter, a pierced silicon wafer etched with traces to distribute the electrical signals to operate the CCDs. A 1.5 m flex cable will be wire-bonded to the pitch adapter a few cm away from the CCD (Fig. 3 left). A transistor used as a signal buffer is directly bonded on the flex at a distance of 40 cm of the CCD. A dedicated R&D was conducted to make the fabrication process of these cable compliant with the low background requirements [11]. The modules will be surrounded with an electro-formed copper can with a low ^{210}Pb content and shielded at the bottom with ancient lead. The CCDs will be assembled into modules in an underground and radon-free ($\sim$ 20mBq/m^3) environment to reduce activation and surface contamination. The estimation of the radioactive

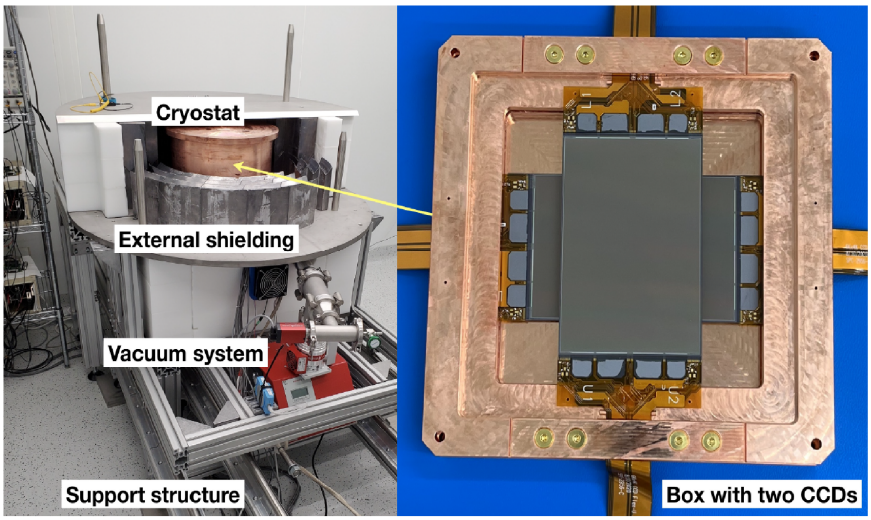

Figure 4: Left: LBC shielding and cryostant assebled on its support structure at LSM. Right: Two CCDs used for the DM electron searches in a copper box.

background yields a total background of 0.6 d.r.u. within the goals now set for DAMIC-M. The major contribution is the ^{210}Pb from the external lead shielding itself [1]. Around 25% can still be attributed to the flex cable and the other subdominant contribution are from the copper can and the inner lead shield.
The electronics chain is composed of the ACM (Acquisition and Control Module) designed for DAMIC-M, a 3 meters cable, a front end board to amplify the video signal, a vacuum interface board to enter in the cryostat and the 1.5 m flex cable. The ACM generates programmable low noise biases with digital potentiometers. Each clocks is produced by two programmable DC levels (with digital to analog converter) chained with a switch to toogle between them. The video signal is amplified on the front end board with commercial low noise amplifier chips and transmitted to the ACM to be digitized by 18 bits and 15 MS/s ADC (analog to digital converter). The local intelligence on the ACM allows to program the operation and readout of the CCD, to process the video signal and to communicate with the data acquisition system.

4. Low Background Chamber DM-electron interaction searches

The Low Background Chamber (LBC) is a prototype detector part of the DAMIC-M developments currently in operation at LSM to demonstrate the performances of CCD and other parts of the final DAMIC-M system to be installed. It was constructed as an intermediate step towards DAMIC-M with a controlled background and is thus able to deliver science results [10].

Detector description The LBC, as operated in 2022, comprises two 6144x4128 pixels CCDs of similar type of the one use for DAMIC-M (except for the size). They are operated at low

[1] the ^{210}Pb concentration used for those simulation are from another ancient lead awaiting for the ongoing assay of the actual one

temperature and pressure and shielded by a two layers of low radioactivity lead and a layer of high density polyethylene as shown in Fig. 4. The radioactive background was estimated to ∼10 d.r.u. which induce negligible background for the searches presented below. The substrate voltage is 70V and a hardware binning, combining 10 rows and 10 columns together is applied during the readout of the CCD to decrease the probability of charge split between pixels (pixels are hereafter considered as 150 µm × 150 µm)

Data selection The interaction of a sub-GeV dark matter particle in a CCD would release a few charges in the crystal. The main source of charge and thus the main background is the thermally or stress induced dark current, the spurious charges induced from clock transition and the absorption of the infra red light emitted by the output amplifier of the CCD. Hence the total amount of background charge is expected to have a spatial dependency and to grow linearly with time. As the skipper readout operation itself takes a sizeable amount of time, the CCD is readout continuously without any static exposure time and the amount of exposed time is related to the size of the image and the number of NDCM. Two data sets acquired with 650 NDCM (corresponding to a resolution of 0.2 e^-) are analysed, Science Run 1 (SR1) and Science Run 2 (SR2) with respectively image size of 640x840 and 640x140 ($N_{col} \times N_{row}$). This translate to an average charge of 0.012 e^-/pixel/image and 0.033 e^-/pixel/image or about 20 e^-/mm^2/day.

Analysis After the charge in each pixel is averaged over the NDCM, the data are subtracted from the pedestal. A calibration constant is found independently for each CCD amplifier by fitting the pixel charge distribution with a Gaussian function convolved with a Poisson distribution. This yields a distribution such as the one in Fig. 2 (right) with separated peaks for 0, 1, and 2e^- . The analysis follows with the identification of clusters of charge and the exclusion of the ones larger than 7 e^- . The 10 trailing pixels in both horizontal and vertical directions are also excluded to account for charge transfer inefficiencies. A search for defects is then conducted by parameterising the 1e-peak as a function of the columns number and exclude any columns with a rate larger than 2σ from this parameterisation. Then, a dedicated data set of 13 images with 3-hour exposure is analysed to identify high charge pixel recurring in multiple images. Finally traps in the serial registers have been identified as columns with a rate lower than the previously mentioned parameterisation by 2 σ. This lead us to exclude one CCD of the analysis and reject pixels with columns > 74 for the second one. The final integrated exposure amounts to 45.26 g.day for SR1 and 39.97 g.days for SR2.

Results As the background charge distribution is not uniform across the CCD array, the background is estimated for every pixel in the data set by fitting only the 0e^- and 1e^- distribution with a Poisson distribution convolved with a Gaussian function to account for the detector energy resolution. The signal distribution is build in three steps: first we estimate the differential event rate from DM-e^- interaction of cross section $\bar{\sigma}_e$ from a DM particle of mass m_χ at a given recoil energy E_e from the parameterisation:

$$\frac{dR}{dE_e} \propto \bar{\sigma}_e \int \frac{dq}{q^2} \eta(m_\chi, q, E_e) |F_{DM}(q)|^2 |f_c(q, E_e)|^2 \tag{1}$$

with q the transferred momentum, η the distribution encoding the properties of the incident galactic DM flux using the astrophysical parameters recommended in [12], $|F_{DM}|$ is a DM form factor

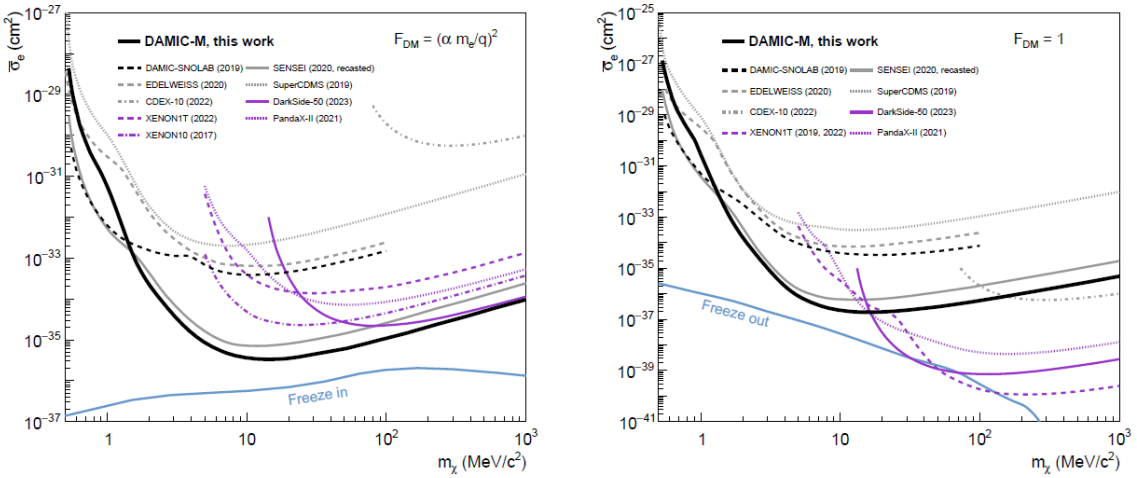

Figure 5: Limits of DM electron cross section as a function of DM mass for ultra light mediator (left) and heavy mediator (right).

which describes the momentum transfer dependence of the interaction and f_c is the crystal form factor which includes the atomic transition probability computed using the QEDark model [15]. Second, the expected ionisation charge is computed thanks to the semi empirical model in [13] and propagated through a simulation of the detector response. Finally we fit the pixel distribution with a function including the signal computed in this way together with a background component convolved with a gaussian function parameterised with the detector resolution.

The result of the background only hypothesis fit is shown together with the pixel charge distribution of one amplifier of the SR2 data set in Fig. 2 (right). The simulation of the pixel charge distribution in simulated for a mass of $m_\chi = 12$ MeV/c^2 and $\bar{\sigma}_e = 2 \times 10^{-37}$ cm^2 is also shown for illustration.

No preference is found for a DM signal and the statistical approach in [16] is used to place limits on DM electron interaction mediated with heavy or ultra light mediator shown in Fig. 5. The world leading limits reflect the low background obtained with the CCD, especially the fact that no pixel with charge larger the 4 e$^-$ (and lower than 7e$^-$) was found in the data set. These searches are compared with other direct detection experiments, in particular the results of SENSEI [17], which use also skipper CCD, are recasted by using the same halo parameters and charge yield model allowing proper comparison. They exclude previously unexplored regions for both cases and are also compared with theoretical model of DM production that reproduce the correct DM abundance (Freeze in and Freeze out curves).

5. Conclusions and future

The effort in the development of DAMIC-M has already yielded several scientifics results [10, 14]. The LBC has also allowed us to set up facilities for DAMIC-M such as slow control system, the clean room environment and procedure, and will soon be host of the new low noise electronics for test in low background environment. The DAMIC-M development have converged into the detector described above hence the construction and the electronics production are expected to start this year

(2023) for a commissioning of the experiment in 2024. DAMIC-M will operate a large quantity of science grade CCDs in an ultra low background environment allowing to further improve this technique and search for DM signal with unprecedented sensitivity.

References

[1] Battaglieri, *et al*. US Cosmic Visions: New Ideas in Dark Matter 2017: Community Report. (2017)

[2] Holland, S. *et al Journal Of Instrumentation*. **9**, C03057 (2014,3)

[3] Aguilar-Arevalo, A. *et al Physical Review Letters*. **125** (2020,12),

[4] Orrell, J *et al Astroparticle Physics*. **99** pp. 9-20 (2018,5)

[5] Aguilar-Arevalo, A. *et al.* arXiv:2306.01717

[6] Chavarria *et al. Physical Review D*. **94**, 082007 (2016,10)

[7] Tiffenberg, J. *et al. Physical Review Letters*. **119** (2017,9)

[8] Aguilar-Arevalo, A., *et al. Physical Review Letters*. **118** (2017,4)

[9] Aguilar-Arevalo, A. *et al. Phys. Rev. D*. **105**, 062003 (2022,3)

[10] Arnquist, I. *et al. Phys. Rev. Lett.*. **130**, 171003 (2023,4),

[11] Arnquist, I. *et al.* arXiv:2303.10862 [physics.ins-det]

[12] Baxter, D. *et al. The European Physical Journal C*. **81** (2021,10)

[13] Ramanathan, K. *et al.Physical Review D*. **102**, 063026 (2020,9)

[14] Norcini, D., *et al. Physical Review D*. **106** (2022,11)

[15] Essig, R. *et al.* J. High Energ. Phys. 2016, 46 (2016)

[16] Cowan, G. *et al.The European Physical Journal C*. **71** (2011,2),

[17] Barak, L. *et al Physical Review Letters*. **125** (2020,10)

Full Authors List: DAMIC-M Collaboration

I. Arnquist[1], N. Avalos[2], D. Baxter[3†], X. Bertou [2], N. Castelló-Mor [4], A.E. Chavarria[5], J. Cuevas-Zepeda[3], A. Dastgheibi-Fard[6], C. De Dominicis [7], O. Deligny[8], J. Duarte-Campderros[4], E. Estrada[2], N. Gadola[9], R. Gaïor[7], T. Hossbach[1], L. Iddir[7], B. Kilminster[9], A. Lantero-Barreda[4], I. Lawson[10], S. Lee [9], A. Letessier-Selvon[7], P. Loaiza[8], A. Lopez-Virto[4], K. J. McGuire[5], P. Mitra[5], S. Munagavalasa[3], D. Norcini[3,11], S. Paul[3], A. Piers[5], P. Privitera[3,7], P. Robmann[9], S. Scorza[6], M. Settimo[12], R. Smida[3], M. Traina[5,7], R. Vilar[4], G. Warot[6], R. Yajur[3], J-P. Zopounidis[7]

[1]Pacific Northwest National Laboratory (PNNL), Richland, WA, United States
[2]Centro Atómico Bariloche and Instituto Balseiro, Comisión Nacional de Energía Atómica (CNEA), Consejo Nacional de Investigaciones Científicas y Técnicas (CONICET), Universidad Nacional de Cuyo (UNCUYO), San Carlos de Bariloche, Argentina
[3]Kavli Institute for Cosmological Physics and The Enrico Fermi Institute, The University of Chicago, Chicago, IL, United States
[4]Instituto de Física de Cantabria (IFCA), CSIC - Universidad de Cantabria, Santander, Spain
[5]Center for Experimental Nuclear Physics and Astrophysics, University of Washington, Seattle, WA, United States
[6]LPSC LSM, CNRS/IN2P3, Université Grenoble-Alpes, Grenoble, France
[7]Laboratoire de physique nucléaire et des hautes énergies (LPNHE), Sorbonne Université, Université Paris Cité, CNRS/IN2P3, Paris, France
[8]CNRS/IN2P3, IJCLab, Université Paris-Saclay, Orsay, France
[9]Universität Zürich Physik Institut, Zürich, Switzerland
[10]SNOLAB, Lively, ON, Canada
[11]Department of Physics and Astronomy, Johns Hopkins University, Baltimore, MD, United States
[12]SUBATECH, Nantes Université, IMT Atlantique, CNRS/IN2P3, Nantes, France

PoS(ICRC2023)1419

[†]Now at Fermi National Accelerator Laboratory, Batavia, IL, United States